ELSEVIER

Chemical Engineering Journal 129 (2007) 123–131

Chemical Engineering Journal

www.elsevier.com/locate/cej

As(III) removal from aqueous medium in fixed bed using iron oxide-coated cement (IOCC): Experimental and modeling studies

Sanghamitra Kundu, A.K. Gupta *

Environmental Engineering Division, Department of Civil Engineering, Indian Institute of Technology, Kharagpur 721302, India

Received 6 May 2006; accepted 11 October 2006

Abstract

Continuous fixed bed studies were undertaken to evaluate the efficiency of iron oxide-coated cement (IOCC) as an adsorbent for the removal of As(III) from aqueous solution under the effect of various process parameters like bed depth (10–20 cm), flow rate (4.3–12 ml min^{-1}) and initial As(III) concentrations (0.5–2.7 mg l^{-1}). The results showed that the total As(III) uptake decreased with increasing flow rate and increased with increasing initial As(III) concentration. Also, the total As(III) removal percentage increased with the increase in bed depth. The dynamics of the adsorption process was modeled by bed depth service time (BDST), mass transfer, Thomas and Yoon–Nelson models. The BDST model fitted well with the experimental data in the initial region of the breakthrough curve but showed slight deviations above break points. Though the experimental data points and the data points predicted using the mass transfer model followed a similar trend, they slightly deviated from each other. The Thomas and Yoon–Nelson model predictions were in very good agreement with the experimental results at all the process parameters studied indicating that they were very suitable for IOCC column design. The apparent mechanism of As(III) removal in the IOCC column were ion exchange and physisorption on the adsorbent surface.

Keywords: Adsorption; Arsenic; Breakthrough curve; BDST model; Mass transfer model; Thomas model; Yoon–Nelson model

1. Introduction

Arsenic is a ubiquitous element in the natural environment that has long affected human life in two contradictory ways as an essential as well as a toxic element. It has been used in humanity's favour as medicine, insecticides, and herbicides and also as a poison since humans first became interested in chemistry [1]. The pesticide sprays began contaminating human foods and environment with arsenic, resulting in serious health risks to humans. However, in recent years, arsenic threatens the drinking water resources in many parts of the world by lurking underground, and the consumption of this tainted water over the years have resulted in unprecedented sufferings of millions of people worldwide.

In natural waters, usually inorganic arsenic in the form of As(III) and/or As(V) is found to be prevalent. Arsenite [As(III)] is much more toxic [2,3] and more soluble and mobile [4] than arsenate [As(V)]. In the pH range of most natural waters (6.5–7.5), As(III) predominantly exists as an uncharged ($H_3AsO_3^0$) specie due to which this form of arsenic is very difficult to be removed by the conventionally applied physico-chemical treatment methods [5] than As(V) [6]. In addition to this, excessive use of chemicals, bulky sludge, and high cost limits their use in small-scale treatment systems. For such systems, fixed-bed treatment processes, such as adsorption, are receiving increasing attention for arsenic removal because of their simplicity, ease of operation and handling, regeneration capacity, and sludge-free operation.

Most of the available literature on arsenic removal by adsorption deal with As(V) removal and very few studies have been reported on As(III) removal in fixed bed [7–10]. Different adsorbents have been developed by researchers for the removal of As(III) from water with various degrees of success. Removal of As(III) from water by adsorption on coconut husk carbon [11], MnO_2 coated sand [12], basic yttrium carbonate [13], activated alumina [14], carbon from fly ash [15], granular titanium dioxide [16], and hybrid polymeric sorbent [17] have been tried. Considering the affinity of arsenic toward iron, various types of iron ores [18], iron oxides [19], iron oxide coated materials [20–24] and also zerovalent iron [25–27] have been effectively used as

* Corresponding author. Tel.: +91 3222 283428; fax: +91 3222 282254.
E-mail address: akgupta@iitkgp.ac.in (A.K. Gupta).

1385-8947/$ – see front matter © 2006 Elsevier B.V. All rights reserved.
doi:10.1016/j.cej.2006.10.014

adsorbents for the removal of both As(III) and As(V) from the aqueous environment. However, most of the reported studies for arsenic removal have been conducted in batch operation and each adsorbent has its merits and demerits in terms of regeneration, adsorbent strength, adsorption capacities of the sorbents, pressure loss during column runs, etc. Batch reactors are very easy to use in the laboratory study, but less convenient for field applications. Moreover, accurate scale-up data for fixed bed systems cannot be obtained from the adsorption isotherms of batch results, so the practical applicability of the adsorbent should be ascertained in column operations. Adsorption on fixed bed columns presents numerous advantages. It is simple to operate, gives high yields and can be easily scaled up from a laboratory process.

Considering the affinity of arsenic towards aluminium and iron, a Ca–Al–Si–Fe–O containing complex substance (iron oxide-coated cement (IOCC)), was used as adsorbent to evaluate its column performance for As(III) removal under continuous flow conditions in a fixed bed mode after promising results were obtained in the batch tests [28]. Breakthrough studies were carried out to evaluate the effect of process parameters, such as the flow rate, bed depth, and influent concentration, on the shape of the breakthrough curve. The dynamics of the adsorption process were modeled by various kinetic models as bed depth service time (BDST) model, mass transfer model, Thomas model and Yoon–Nelson model.

2. Analysis of column data

2.1. Mathematical analysis

The loading behaviour of As(III) to be removed from solution in a fixed bed containing the IOCC media are shown by breakthrough curves that are expressed in terms of normalized concentration defined as the ratio of effluent As(III) concentration to inlet As(III) concentration (C_t/C_0) as a function of time (t) or volume of effluent (V_{eff}) for a given bed height (h). The volume of the effluent (V_{eff}) can be calculated from the following equation:

$$V_{\text{eff}} = Qt_{\text{tot}} \tag{1}$$

where Q is the volumetric flow rate (ml min^{-1}) and t_{tot} is the total time of flow till exhaust (min), respectively. The total adsorbed As(III) quantity (q_{tot}; mg) in the column for a given feed concentration (C_0) and flow rate (Q) can be found by calculating the area under the breakthrough curve (A) which is obtained by integrating the adsorbed As(III) concentration (C_{ads} (mg l^{-1}) = inlet As(III) concentration (C_0) − effluent As(III) concentration (C_t)) versus time t (min) plot (Eq. (2))

$$q_{\text{tot}} = \frac{QA}{1000} = \frac{Q}{1000}\int_{t=0}^{t=\text{tot}} C_{\text{ads}}\,\mathrm{d}t \tag{2}$$

The total amount of As(III) fed to the column (X; mg) is calculated from the following equation:

$$X = \frac{C_0 Q t_{\text{tot}}}{1000} \tag{3}$$

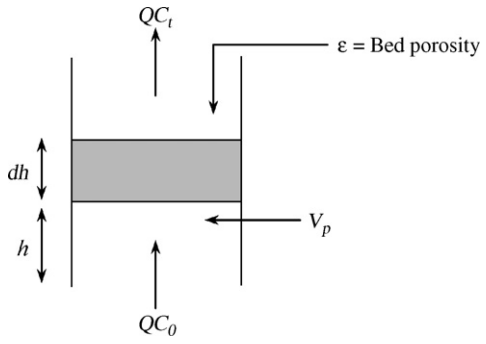

Fig. 1. Scheme of bed depth [29].

The total percent removal of As(III) by the column, i.e. the column performance by IOCC can be calculated from the following equation:

$$\text{total As(III) removal (\%)} = \frac{q_{\text{tot}}}{X} \times 100 \tag{4}$$

2.2. Modeling of breakthrough curves

Prediction of the breakthrough curve for the effluent is the predominant factor for the successful design of a column adsorption process. It is innately difficult to develop a model which accurately describes the dynamic behaviour of adsorption in a fixed bed system. The process does not operate in a steady state as the concentration of the adsorbate changes as the feed moves through the bed. The fundamental transport equations for a fixed bed are those of material balance between the solid and fluid. Fig. 1 illustrates the variation of this balance during the reaction. The equation of mass balance material can be stated as: input flow = output flow + flow inside pore + matter adsorbed onto the bed.

The mass balance material equation for this system can be expressed mathematically as

$$\frac{QC_0}{1000} = \frac{QC_t}{1000} + V_{\text{p}}\frac{\mathrm{d}C}{\mathrm{d}t} + m\frac{\mathrm{d}q}{\mathrm{d}t} \tag{5}$$

where QC_0 is the inlet flow of As(III) in the column (mg min^{-1}), QC_t the outlet flow of As(III) leaving the column (mg min^{-1}), V_{p} the porous volume (l) ($V_{\text{p}} = (1/(1-\varepsilon))V$ where V is the bulk volume (l) and ε is the void fraction in the bed), $V_{\text{p}}(\mathrm{d}C/\mathrm{d}t)$ the flow rate through the column bed depth (mg min^{-1}) and $m(\mathrm{d}q/\mathrm{d}t)$ the amount of As(III) adsorbed onto IOCC (mg min^{-1}) where m is the mass of IOCC (g) and $\mathrm{d}q/\mathrm{d}t$ is the adsorption rate (mg g^{-1} min^{-1}).

From the above relation (Eq. (5)), it is evident that the linear flow rate ($u = Q/S_{\text{c}}$, where S_{c} is the column section, m^2), the initial solute concentration, the adsorption potential and the porous volume are the determining factors of the balance for a given column bed depth. Therefore, it is necessary to examine these parameters and to estimate their influence in order to optimize the fixed bed column adsorption process. However, these equations derived to model the fixed bed adsorption system with theoretical vigor are differential in nature and usually require complex numerical methods to solve them. Because of

this, various simple numerical models have been developed to predict the dynamic behaviour of the columns and some of these models have been discussed here. The prediction and analysis of the dynamic behaviour of the column was carried out with the bed depth service time (BDST) model, mass transfer model, Thomas model and Yoon–Nelson model. The average percentage errors between the experimental and predicted values were calculated using the following equation:

$$E\% = \frac{\sum_{i=1}^{N} |((C_t/C_0)_{\text{exp}} - (C_t/C_0)_{\text{theo}})/(C_t/C_0)_{\text{exp}}|}{N} \times 100 \quad (6)$$

2.2.1. The bed depth service time (BDST) approach

The BDST model, proposed by Hutchins [30], describes a relation between the service time and the packed-bed depth of the column and is expressed as

$$C_0 t = \frac{N_0 h}{u} - \frac{1}{K} \ln\left[\frac{C_0}{C_t} - 1\right] \quad (7)$$

where C_0 is the influent concentration (mg l^{-1}), C_t the effluent concentration at time t (mg l^{-1}), K the adsorption rate constant (l mg^{-1} min^{-1}), N_0 the adsorption capacity (mg l^{-1}), h the bed depth of IOCC (cm), u the linear flow rate (cm min^{-1}) and t is the service time to breakthrough (min).

Experimental data obtained were used to plot BDST curves and estimate the characteristic parameters, K and N_0 from the slope and intercept of the plots.

2.2.2. The mass transfer model

Using the data obtained from the batch isotherm studies, it is possible to predict the theoretical breakthrough curve, which can be well compared with the experimental curve. The theoretical breakthrough curve was generated following the concept presented by Michaels [31]. The detailed calculations for the generation of the experimental breakthrough curve from the equilibrium data obtained from batch studies are as follows:

1. Firstly, an experimental equilibrium curve was drawn assuming various values of C_e (equilibrium concentration of As(III) remaining in the solution (mg l^{-1})) and calculating the corresponding values of q_e (amount of As(III) (mg) adsorbed per unit weight of IOCC (g)) using the best fit isotherm model obtained from the batch results.
2. An operating line can then be constructed by considering an adsorbate materials balance over the column [32]. The amount of As(III) on the IOCC media is related to the amount As(III) in solution by

$$q_t = \frac{C_t}{C_0}[q_0 - q_r] + q_r \quad (8)$$

where q_t is the amount of As(III) on IOCC (mg g^{-1}), q_0 the equilibrium As(III) uptake per gram of IOCC (mg g^{-1}) and q_r is the residual amount of As(III) on IOCC after regeneration (mg g^{-1}).

Assuming that fresh IOCC medium is used, q_r is initially equal to zero and Eq. (8) becomes

$$q_t = \frac{C_t}{C_0} q_0 \quad (9)$$

Thus, when $C_t = C_0$, q_t is equal to q_0, and the coordinate (C_0, q_0) represents a point on the operating line. Since the operating line must also pass through the origin, the other coordinate is (0, 0).

3. According to Weber [33], the rate of transfer of solute from solution over a differential depth of column, dh, is given by

$$F_w \, dC = K_a (C - C^*) \, dh \quad (10)$$

where F_w is the wastewater flow rate, K_a the overall mass transfer coefficient, which includes the resistances offered by film diffusion and pore diffusion and C^* is the equilibrium concentration of solute in solution corresponding to an adsorbed concentration, q_e.

The term $(C - C^*)$ is the driving force for adsorption and is equal to the distance between the operating line and equilibrium curve at any given value of q_e. Integrating Eq. (10) and solving for the height of the adsorption zone,

$$h_z = \frac{F_w}{K_a} \int_{C_B}^{C_E} \frac{dC}{C - C^*} \quad (11)$$

For any value of h less than h_z, corresponding to a concentration C between C_B and C_E, Eq. (11) can be written as

$$h = \frac{F_w}{K_a} \int_{C_B}^{C} \frac{dC}{C - C^*} \quad (12)$$

Dividing Eq. (12) by Eq. (11) results in

$$\frac{h}{h_z} = \frac{\int_{C_B}^{C} dC/(C - C^*)}{\int_{C_B}^{C_E} dC/(C - C^*)} = \frac{V - V_B}{V_E - V_B} \quad (13)$$

where V_B and V_E are total volume of water treated till breakthrough and up to exhaust point, respectively, and V is the volume of water treated within V_E for effluent concentration C with in C_E. Dividing the values of $\int_{C_B}^{C} dC/(C - C^*)$ by the value of $\int_{C_B}^{C_E} dC/(C - C^*)$ the term $(V - V_B)/(V_E - V_B)$ was evaluated.

4. Now the plot of C/C_0 versus $(V - V_B)/(V_E - V_B)$ represents the theoretical breakthrough curve.

2.2.3. The Thomas model

The expression developed by Thomas [34] calculates the maximum solid phase concentration of solute on the sorbent and the adsorption rate constant for an adsorption column. The linearized form of the model is given as:

$$\ln\left(\frac{C_0}{C_t} - 1\right) = \frac{k_{Th} q_0 m}{Q} - \frac{k_{Th} C_0 V_{eff}}{Q} \quad (14)$$

where k_{Th} is the Thomas rate constant (ml min^{-1} mg^{-1}), q_0 the equilibrium As(III) uptake per gram of the adsorbent (mg g^{-1}) and m is the amount of adsorbent in the column (g).

The kinetic coefficient k_{Th} and the adsorption capacity of the column q_0 can be determined from a plot of $\ln((C_0/C_t) - 1)$ against t ($=V_{eff}/Q$) at a given flow rate.

2.2.4. The Yoon–Nelson model

The Yoon and Nelson [35] model is based on the assumption that the rate of decrease in the probability of adsorption for each adsorbate molecule is proportional to the probability of adsorbate adsorption and the probability of adsorbate breakthrough on the adsorbent. The linearized model for a single component system is expressed as

$$\ln \frac{C_t}{C_0 - C_t} = k_{YN}t - \tau k_{YN} \quad (15)$$

where k_{YN} is the rate constant (min^{-1}) and τ is the time required for 50% adsorbate breakthrough (min).

The calculation of theoretical breakthrough curves for a single-component system requires the determination of the parameters k_{YN} and τ for the adsorbate from the plot of $\ln[C_t/(C_0 - C_t)]$ versus sampling time (t) according to Eq. (15).

3. Materials and methods

The IOCC adsorbent used in the present study was prepared according to the method described by Kundu and Gupta [36]. Its chemical composition (as oxides in wt%) was CaO 55.11%, Fe-oxide 23.53%, Al_2O_3 11.06%, quartz 9.72% and MgO 0.58%. The XRD pattern of IOCC showed predominant peaks of $Ca(OH)_2$, calcium–silicate–hydrate (C–S–H) and Fe_3O_4. The bulk density and porosity were found to be 1.43 g cm^{-3} and 0.56 fraction, respectively. The iron leaching from the media was found to be very insignificant and in the range of 0.018–0.02 mg l^{-1}.

All the chemicals used in the study were of analytical grade and used without further purification. Double distilled water was used in preparation of all the solutions. Arsenite [As(III)] stock solutions (1000 mg l^{-1}) were prepared by dissolving $NaAsO_2$ (LOBA Chemie) in double distilled water from which working solutions, as per the experimental requirements, were freshly prepared for each experimental run.

The concentration of arsenic in the effluent was determined spectrophotometrically using UV–vis spectrophotometer (Thermospectronic, Model no. UV-1, UK), at a wavelength of 535 nm, by the silver dithiodiethylcarbamate method (minimum detectable quantity: 1 μg As) after [37].

Continuous fixed bed adsorption studies were performed in a borosilicate glass column (internal diameter: 20 mm, length: 550 mm), packed with IOCC between two supporting layers of glass wool (Fig. 2), to evaluate the column performance of IOCC in removing As(III). The As(III) solution at a known concentration and flow rate was charged continuously through the stationary IOCC bed in the up-flow mode. The influent feed flow rate was regulated and maintained with a variable flow peristaltic pump (Miclins, India). Effluent samples were taken at pre-determined time intervals and analyzed for As(III). The experiments were continued until a constant As(III) concentration was obtained. The breakthrough concentration of As(III) was taken as 0.01 mg l^{-1} according to the permissible limit in drinking water set by the WHO [38] standards. The exhaust concentration was taken as 90% of the inlet As(III) concentration, i.e., $0.9C_0$.

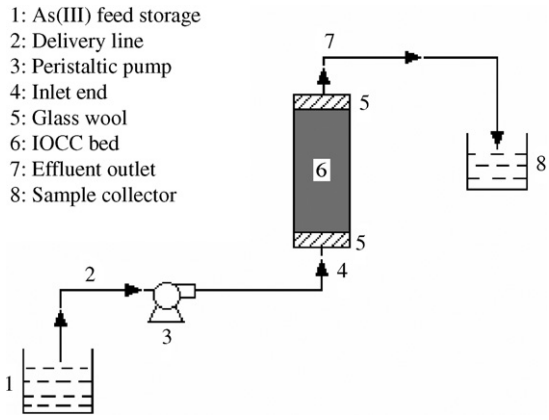

Fig. 2. Experimental setup for fixed bed operation.

All the experiments were carried out at room temperature ($27 \pm 2\,^{\circ}C$) and atmospheric pressure and no pH adjustments were made.

The effects of various process parameters viz. bed depth (h = 10–30 cm, C_0 = 1.35 mg l^{-1}, Q = 8.5 ml min^{-1}), inlet As(III) concentration (C_0 = 0.5–2.7 mg l^{-1}, h = 10 cm, Q = 8.5 ml min^{-1}), flow rate (Q = 4.3–12 ml min^{-1}, h = 10 cm, C_0 = 1.35 mg l^{-1}) were investigated to evaluate the performance of breakthrough on As(III) adsorption by IOCC.

4. Results and discussion

For fixed bed column operations for As(III) removal by IOCC bed, the As(III) spiked water was passed through the fixed bed in the up-flow mode. During the adsorption experiments, it was observed that the flow rate remained more or less constant which indicated that the clogging of pores did not occur and hence, the sorption sites of IOCC particles were easily accessible through the interparticle pore network. The pH of the effluent ranged from 8.5 to 9. This is probably because of the release of some amount of Ca^{2+} in the form of $Ca(OH)_2$ from the adsorbent material. However, the concentration of Ca^{2+} in the effluent was found to be within the taste threshold (100–300 mg l^{-1}) set by WHO [39].

The shape of the breakthrough curve and the time for the breakthrough appearance are the predominant factors for determining the operation and the dynamic response of an adsorption column. The general position of the breakthrough curve along the volume/time axis depends on the capacity of the column with respect to bed height, the feed concentration and flow rate.

4.1. Effect of bed depth

The breakthrough curves obtained for As(III) adsorption onto IOCC at different bed depths (10, 20, and 30 cm), at a constant linear flow rate of 2.706 cm min^{-1} and 1.35 mg l^{-1} initial As(III) concentration are shown in Fig. 3. The results indicate that the

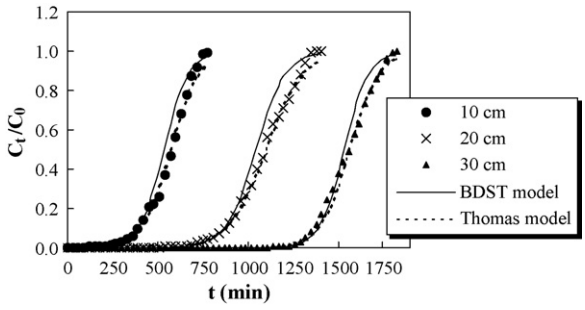

Fig. 3. Measured and modeled breakthrough profiles of As(III) adsorption onto IOCC at different bed depths ($Q = 8.5$ ml min^{-1}, $C_0 = 1.35$ mg l^{-1}).

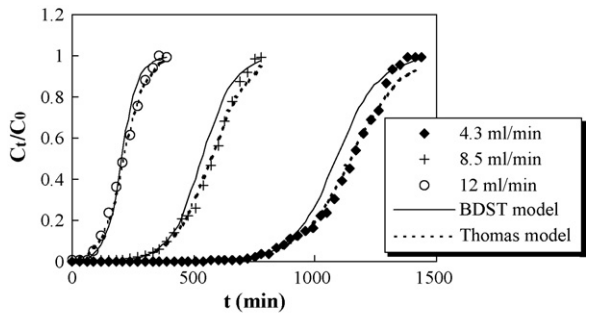

Fig. 4. Measured and modeled breakthrough profiles of As(III) adsorption onto IOCC at different flow rates ($C_0 = 1.35$ mg l^{-1}, $h = 10$ cm).

volume of breakthrough varies with bed depth (Table 1). The bed capacity, percent removal of As(III) and exhaustion time (corresponding to an effluent concentration = $0.9C_0$) increased with increasing bed height, as more binding sites were available for sorption. The increase in adsorption with bed depth was due to the increase in adsorbent doses in larger beds which provided greater adsorption sites for As(III). The breakthrough time also increased with the bed depth, suggesting that it is the determining parameter of the process (Table 1). The larger the breakthrough time, better is the intra-particulate phenomena.

4.2. Effect of flow rate

The effect of flow rate on As(III) adsorption by IOCC was investigated by varying the flow rate from 4.3 to 12 ml min^{-1} and keeping the initial As(III) concentration (1.35 mg l^{-1}), bed depth (10 cm) and column diameter (2 cm) constant. The plot of normalized As(III) concentration versus time at various flow rates is shown in Fig. 4. The total sorbed As(III) quantities, treated volume at breakthrough, breakthrough times and As(III) removal percents with respect to flow rate were evaluated from the sorption data and are presented in Table 1. As is evident from the results presented in Table 1, an increase in the flow rate reduces the volume treated efficiently until breakthrough and thereby decreases the service time of the bed. This is due to the decrease in the residence time of the As(III) ions within the bed at higher flow rates. Much sharper breakthrough curves for As(III) adsorption onto IOCC were obtained at higher flow rates. The breakthrough time and the amount of total As(III) adsorbed also decreased with increasing flow rate. This is certainly because of the reduced contact time causing a weak distribution of the liquid inside the column, which leads to a lower diffusivity of the solute among the particles of the adsorbent. Zouboulis and Katsoyiannis [9] who studied arsenic removal using iron oxide loaded alginate beads also reported that the fact that sorbate adsorption increases with increasing the sorbate residence time in the column indicating that adsorption is controlled by sorbate mass transfer into the adsorbent.

4.3. Effect of initial As(III) concentration

The sorption performance of IOCC was investigated at different initial As(III) concentrations. The effect of varying the initial As(III) concentrations from 0.5 to 2.7 mg l^{-1} at a flow rate of 8.5 ml min^{-1} and bed depth 10 cm are illustrated in Fig. 5. The total sorbed As(III) quantities, treated volume at breakthrough,

Table 1
Adsorption data for fixed bed IOCC column for As(III) adsorption at different process parameters

Process parameters	Treated volume, V_b (ml)	Breakthrough time, t_b (min)	Total As(III) sorbed, q_{tot} (mg)	Total As(III) removal (%)
Bed depth, h (cm)[a]				
10 ($m = 23.5$ g)	1,785	210	6.453	72.10
20 ($m = 47$ g)	5,610	660	12.457	76.99
30 ($m = 70$ g)	10,285	1210	17.802	84.77
Flow rate, Q (ml min^{-1})[b]				
4.3	2,709	630	6.567	78.56
8.5	1,785	210	6.453	72.10
12	720	60	3.414	54.04
Initial concentration, C_0 (mg l^{-1})[c]				
0.5	4,290	504.7	5.839	75.08
1.35	1,785	210	6.453	72.10
1.9	990	116.47	6.838	70.57
2.7	615	72.36	7.153	61.11

Breakthrough concentration = 0.01 mg l^{-1}.
[a] $C_0 = 1.35$ mg l^{-1}, $u = 2.706$ cm min^{-1}, $Q = 8.5$ ml min^{-1}.
[b] $C_0 = 1.35$ mg l^{-1}, $h = 10$ cm, $m = 23.5$ g.
[c] $Q = 8.5$ ml min^{-1}, $h = 10$ cm, $m = 23.5$ g.

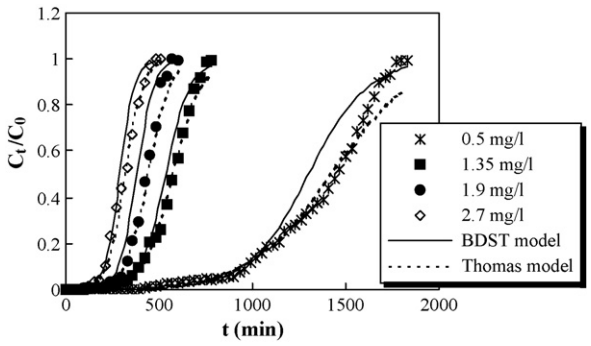

Fig. 5. Measured and modeled breakthrough profiles of As(III) adsorption onto IOCC at different initial As(III) concentrations ($Q = 8.5$ ml min^{-1}, $h = 10$ cm).

breakthrough times and removal percents with respect to the initial As(III) concentration were evaluated from the sorption data and are presented in Table 1. As is evident from Table 1, with the rise in the initial As(III) concentration the volume of solution treated before breakthrough reduces considerably. This is due to the fact that a high sorbate concentration easily saturates the column bed, thereby decreasing the breakthrough time. The amount of total sorbed As(III) increases from 5.839 to 7.153 mg with the rise in the As(III) concentration from 0.5 to 2.7 mg l^{-1} quite contrary to the As(III) removal percentages which exhibit an opposite trend. The total As(III) removal percentage decreased from 75.08 to 61.11% with the increase in inlet As(III) concentration from 0.5 to 2.7 mg l^{-1}. The main driving force for the adsorption process is the concentration difference between the solute in the solution and the solute on the sorbent [40]. This may explain the reason why higher sorbed As(III) quantities were obtained at higher As(III) feed concentrations.

4.4. Application of the BDST model

The BDST sorption model was applied to the experimental data to study the breakthrough behaviour of As(III) onto IOCC and to estimate the characteristic parameters, K and N_0 from the model. Applying Eq. (7) to the experimental data at different bed depths, inlet As(III) concentrations and flow rates, a linear relationship between $\ln((C_0/C_t) - 1)$ and $C_0 t$ was obtained for the relative concentration range up to exhaust, for all breakthrough curves ($R^2 > 0.91$). The respective values of K and N_0 calculated from the slope and intercept of the linear plot are presented in Table 2. From the table it is evident that the maximum adsorption capacity N_0 decreased with the increase in bed depth and flow rate, and increased with the increase in the initial As(III) concentration. The values of the adsorption rate constants were influenced by flow rate and increased with increase in flow rate indicating that external mass transfer dominated the overall system kinetics was in the initial part of the adsorption in the column. The breakthrough curves predicted from the BDST model were compared with the experimental breakthrough curves and are shown in Figs. 3–5. It is clear from the figures that though the model fits well in the initial region of the breakthrough curve, there are slight discrepancies between the BDST predicted and experimental values above break points. This indicates that though the BDST model provides a simple and comprehensive approach for evaluating sorption column test, its validity is limited in the range of conditions used [41–43].

4.5. Application of the mass transfer model based on batch isotherm studies to the experimental data

Following the mass transfer model approach, theoretical breakthrough curve was generated using the data obtained from batch isotherm studies, which was then compared with the experimental breakthrough curve. Assessing the best fit isotherm from the magnitude of the correlation coefficient obtained by fitting the batch experimental results to the linearised Freundlich and Langmuir isotherms, it was found that Langmuir isotherm ($R^2 = 0.999$) provided a better fit compared to Freundlich isotherm ($R^2 = 0.994$). So the Langmuir isotherm equation obtained from the batch isotherm studies ($q_e = 0.276C_e/(1 + 0.4C_e)$) was used to generate the theoretical breakthrough curve, for an initial As(III) concentration of 1.35 mg l^{-1}. Fig. 6 shows the generated breakthrough curve in comparison with the experimental breakthrough curve corresponding to 30 cm bed depth. Though the predicted and the experimental curves follow a somewhat similar trend, the data points deviate from each other. This is due to the fact that the data from batch equilibrium experiments have been transformed into a theoretical breakthrough curve. It is an expected fact that the values of the isotherm parameters obtained in a batch system will be different and considerably higher from those obtained in a fixed bed system, as the solution flow rate in batch system is zero. In other words, the contact time between the sorbate and the sorbent in a batch system is infinite.

Table 2
BDST model parameters for As(III) adsorption onto IOCC at different bed depths, inlet As(III) concentration and flow rates

C_0 (mg l^{-1})	h (cm)	Q (ml min^{-1})	u	K	N_0	R^2	ε (%)
0.5	10	8.5	2.705	0.0125	175.8818	0.9111	30.3
1.35	10	4.3	1.368	0.0083	200.6993	0.9655	23.5
1.35	10	8.5	2.705	0.0112	195.6716	0.9636	19.0
1.35	10	12	3.818	0.0214	105.7051	0.9675	23.1
1.35	20	8.5	2.705	0.0091	190.8378	0.9541	20.6
1.35	30	8.5	2.705	0.0111	186.7622	0.9668	15.0
1.9	10	8.5	2.705	0.0117	195.9773	0.9155	50.8
2.7	10	8.5	2.705	0.0095	213.1729	0.9628	19.3

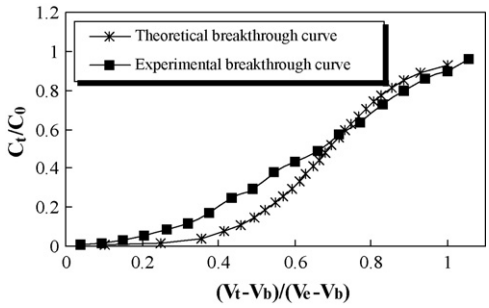

Fig. 6. Measured and predicted breakthrough curve according to the mass transfer model ($C_0 = 1.35\ \mathrm{mg\,l^{-1}}$).

4.6. Application of the Thomas model

The Thomas model was fitted to the column data to investigate the breakthrough behaviour of As(III) onto IOCC. Application of the Thomas model to the data in the concentration (C_t) range of $0.01\ \mathrm{mg\,l^{-1}} < C_t < 0.9C_0$ with respect to bed depth, initial As(III) concentration and flow rate helped in the determination of the Thomas' kinetic coefficients for this system. The coefficients were determined from the slope and intercepts obtained from the linear regression performed on each set of transformed data. Analysis of the regression coefficients indicated that the regressed lines provided excellent fits to the experimental data with R^2 values ranging from 0.9731 to 0.9974 (Table 3). Table 3 also presents the values of k_{Th} and q_0. The bed capacity q_0 decreased and the coefficient k_{Th} increased with increasing flow rates. On the other hand, with the increase in the initial As(III) concentration, the values of q_0 increased and that of k_{Th} decreased. As is evident from Table 3, the differences between the experimental and predicted values of bed capacity (q_0) were negligible at all the operating conditions studied. Figs. 3–5 shows the comparison of the breakthrough curves obtained experimentally with those predicted using the Thomas model at various operating conditions. It is clear from all the figures that the model predicted normalized concentration values were in very good agreement with the experimental values at all As(III) concentrations at all operating conditions.

4.7. Application of the Yoon–Nelson model

The simple Yoon–Nelson model was applied to investigate the breakthrough behaviour of As(III) onto IOCC fixed bed. This model introduces the parameter τ, which shows the treatment time taken for C_t (effluent exit concentration) to be half the initial concentration ($C_0/2$). The values of the model parameters k_{YN} (rate constant) and τ were determined from the slope and intercepts of the linear plots of $\ln[C_t/(C_0 - C_t)]$ versus time t with respect to bed depth, initial As(III) concentration and flow rate and are presented in Table 4. The experimental data exhibited good fits to the model with linear regression coefficients ranging from 0.9744 to 0.9951 (Table 4). As is evident from the table the experimental and the calculated τ-values are very close to each other indicating that the Yoon–Nelson model fits excellently to the experimental data. Comparison of breakthrough curves obtained experimentally with those predicted using the Yoon–Nelson model are shown in Figs. 7–9. The results in the figures clearly indicate that the model proposed by Yoon–Nelson provided a very good correlation with the experimental normalized concentration values at all As(III) concentrations and at all operating conditions.

Table 3
Predicted Thomas model parameters and their deviation from experimental values for As(III) adsorption onto IOCC at different bed depths, inlet As(III) concentration and flow rates

C_0 ($\mathrm{mg\,l^{-1}}$)	h (cm)	Q ($\mathrm{ml\,min^{-1}}$)	k_{Th} ($\mathrm{ml\,mg^{-1}\,min^{-1}}$)	$q_{0,\mathrm{cal}}$ ($\mathrm{mg\,g^{-1}}$)	$q_{0,\mathrm{exp}}$ ($\mathrm{mg\,g^{-1}}$)	R^2	ε (%)
0.5	10	8.5	9.2	0.2565	0.2478	0.9731	20.6
1.35	10	4.3	7.111	0.2821	0.2791	0.9889	11.3
1.35	10	8.5	9.629	0.2782	0.2745	0.9934	10.0
1.35	10	12	16.074	0.1462	0.1452	0.9923	51.4
1.35	20	8.5	7.185	0.2679	0.2649	0.9974	16.2
1.35	30	8.5	9.259	0.2559	0.2542	0.9848	18.9
1.9	10	8.5	9.316	0.3006	0.2902	0.9901	20.7
2.7	10	8.5	7.963	0.3082	0.3039	0.9835	14.9

Table 4
Predicted Yoon–Nelson model parameters and their deviation from experimental values for As(III) adsorption onto IOCC at different bed depths, inlet As(III) concentration and flow rates

C_0 ($\mathrm{mg\,l^{-1}}$)	h (cm)	Q ($\mathrm{ml\,min^{-1}}$)	k_{YN} ($\mathrm{l\,min^{-1}}$)	τ_{cal} (min)	τ_{exp} (min)	R^2	ε (%)
0.5	10	8.5	0.0046	1411.7	1454	0.9744	21.5
1.35	10	4.3	0.0097	1131.2	1156	0.9909	13.1
1.35	10	8.5	0.0131	566.7	579	0.9935	10.2
1.35	10	12	0.0253	215.1	214	0.9776	24.9
1.35	20	8.5	0.0103	1095.5	1092	0.9951	11.2
1.35	30	8.5	0.0131	1553.9	1564	0.9899	15.4
1.9	10	8.5	0.0167	434.2	429	0.9794	22.5
2.7	10	8.5	0.0213	316.4	321	0.991	15.3

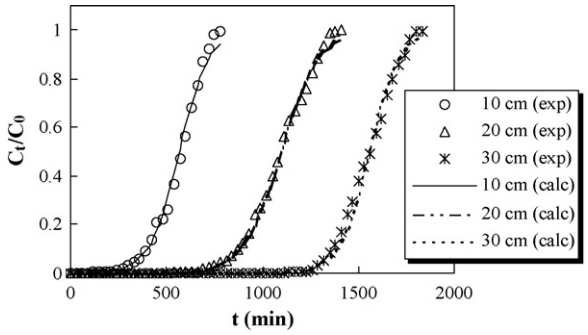

Fig. 7. The measured and modeled breakthrough curves for As(III) adsorption onto IOCC at different IOCC bed depths according to the Yoon–Nelson model ($Q = 8.5\ \mathrm{ml\ min^{-1}}$, $C_0 = 1.35\ \mathrm{mg\ l^{-1}}$).

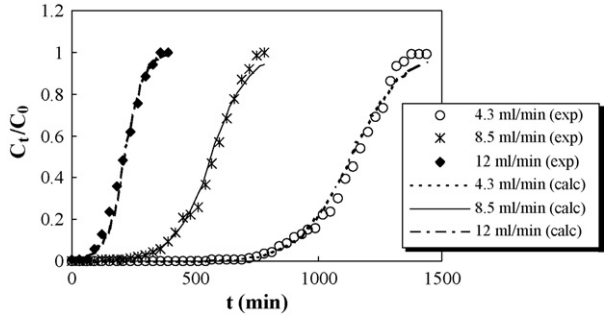

Fig. 8. The measured and modeled breakthrough curves for As(III) adsorption onto IOCC at different flow rates according to the Yoon–Nelson model ($C_0 = 1.35\ \mathrm{mg\ l^{-1}}$, $h = 10$ cm).

4.8. As(III) removal mechanism

The column results suggest a good uptake of As(III) by IOCC. In the pH range of 6.5–7.5, As(III) predominantly exists as an uncharged ($H_3AsO_3{}^0$) specie. However, at an alkaline pH range of 7.5–9.0, this uncharged specie dissociates as $H_3AsO_3{}^0 = H_2AsO_3{}^- + H^+$. As stated earlier, the adsorbent's pH in water is 8.5–9, which assists in this dissociation. Judging by the nature of IOCC media, it is difficult to identify which active surface specie (calcium–silicate–hydrate or C–S–H, Fe_3O_4) is responsible for the As(III) removal. However, some possible interactions that may be occurring within the media and the feed are presented as follows:

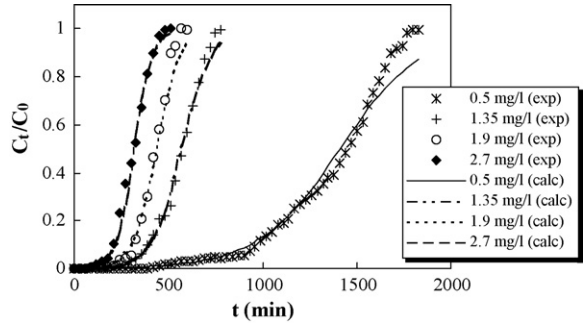

Fig. 9. The measured and modeled breakthrough curves for As(III) adsorption onto IOCC at different initial As(III) concentrations according to the Yoon–Nelson model ($Q = 8.5\ \mathrm{ml\ min^{-1}}$, $h = 10$ cm).

1. The H^+ released on dissociation of $H_3AsO_3{}^0$ are electrostatically attracted by the lone pair of O-atoms, which are bridged between two Fe-atoms in Fe_3O_4, as

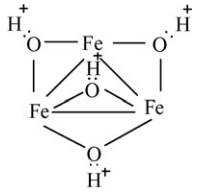

thereby forming an adsorption site for the charged $H_2AsO_3{}^-$. Adsorption of the $H_2AsO_3{}^-$ onto the medium then occurs as

$$[Fe_3(OH)_4]^{4+} + H_2AsO_3{}^- \rightarrow [Fe_3(OH{-}H_2AsO_3)_4] \quad (16)$$

2. The dissociated $H_2AsO_3{}^-$ ion may interact with the other surface specie C–S–H to undergo complex formation reactions in the following manner:

$$(Si{-}O^-)_2Ca^{2+} + H_3O^+ \rightarrow 2(Si{-}OH) + Ca^{2+} + OH^- \quad (17)$$

$$2Si{-}OH + 2H_2AsO_3{}^- \rightarrow 2Si{-}H_2AsO_3 + OH^- \quad (18)$$

Reactions (16–18) probably occur before breakthrough when the As(III) is completely removed. Thus the apparent mechanisms for As(III) removal from IOCC column are physisorption and ion exchange.

5. Conclusion

Experimental and theoretical investigations were carried out on As(III) adsorption from aqueous solution onto IOCC in a continuous fixed bed column at various bed depths, flow rates and initial As(III) concentrations. The results obtained are as follows:

- These studies show that iron oxide-coated cement (IOCC) is an effective adsorbent in removing As(III) from the aqueous environment.
- The sorption of As(III) is strongly dependent on the bed depth, flow rate and initial As(III) concentration. With the increase in flow rate the breakthrough curves became steeper, the breakthrough time and As(III) removal % decreased. The total quantity of As(III) adsorbed increased with the increase in inlet As(III) concentration but removal percentage decreased.
- The effectiveness of the IOCC column increased when lower flow rates and higher bed depths were used.
- The breakthrough data predictions by the BDST approach slightly deviated from the experimental results above breakpoint due to complexity of the adsorption process.
- The mass transfer model could not provide a very good correlation between the data obtained from the batch and the column experiments.
- The Thomas and Yoon–Nelson models provided very good descriptions of the breakthrough curves at all the process parameters studied and were proposed for use in column design.

- The mechanism of lead removal in GBFS column includes ion exchange and physisorption.

References

[1] K. Shiomi, Arsenic in marine organisms: chemical forms and toxicological aspects, in: J.O. Nriagu (Ed.), Arsenic in the Environment. Part II. Human Health and Ecosystem Effects, John Wiley & Sons, Inc., New York, 1994, pp. 261–282.

[2] J.F. Ferguson, J. Gavis, A review of the arsenic cycle in natural waters, Water Res. 6 (1972) 1259–1274.

[3] J.L. Webb (Ed.), Enzyme and Metabollic Inhibitors, Academic Press, New York, 1976.

[4] L.E. Deuel, A.R. Swoboda, Arsenic solubility in a reduced environment, Soil Sci. Soc. Am. Proc. 36 (1972) 276–278.

[5] M.R. Jekel, Removal of arsenic in drinking water treatment, in: J.O. Nriagu (Ed.), Arsenic in the Environment. Part I. Cycling and Characterization, Wiley-Interscience, New York, 1994, pp. 119–130.

[6] F.W. Pontius, G.K. Brown, J.C. Chien, Health implications of arsenic in drinking water, J. Am. Water Works Assoc. 86 (1994) 52–63.

[7] R.C. Vaishya, S.K. Gupta, Modeling arsenic(V) removal from water by sulfate-modified iron oxide coated sand (SMIOCS), Sep. Sci. Technol. 39 (2004) 641–666.

[8] R.C. Vaishya, S.K. Gupta, I.C. Agarwal, Fixed-bed modelling of arsenic(III) adsorption from water by sulfate modified iron oxide coated sand (SMIOCS), in: Proceedings of the 12th International Conference on Heavy Metals in the Environment, J. Phys. IV 107 (2003) 1325–1328.

[9] A.I. Zouboulis, I.A. Katsoyiannis, Arsenic removal using iron oxide loaded alginate beads, Ind. Eng. Chem. Res. 41 (2002) 6149–6155.

[10] T.S. Singh, K.K. Pant, Experimental and modeling studies on fixed bed adsorption of As(III) ions from aqueous solution, Sep. Purif. Technol. 48 (2006) 288–296.

[11] G.N. Manju, C. Raji, T.S. Anirudhan, Evaluation of coconut husk carbon for the removal of arsenic from water, Water Res. 32 (1998) 3062–3070.

[12] S. Bajpai, M. Chaudhuri, Removal of arsenic from groundwater by manganese dioxide-coated sand, J. Environ. Eng.-ASCE 125 (1999) 782–784.

[13] S.A. Wasay, Md. J. Haron, A. Uchiumi, S. Tokunaga, Removal of arsenite and arsenate ions from aqueous solution by basic yttrium carbonate, Water Res. 30 (1996) 1143–1148.

[14] T.S. Singh, K.K. Pant, Equilibrium, kinetics and thermodynamic studies for adsorption of As(III) on activated alumina, Sep. Purif. Technol. 36 (2004) 139–147.

[15] J. Patanayak, K. Mondal, S. Mathew, S.B. Lalvani, A parametric evaluation of the removal of As(V) and As(III) by carbon-based adsorbents, Carbon 38 (2000) 589–596.

[16] S. Bang, M. Patel, L. Lippincott, X. Meng, Removal of arsenic from groundwater by granular titanium dioxide adsorbent, Chemosphere 60 (2005) 389–397.

[17] M.J. DeMarco, A.K. Sengupta, J.E. Greenleaf, Arsenic removal using a polymeric/inorganic hybrid sorbent, Water Res. 37 (2003) 164–176.

[18] D.B. Singh, G. Prasad, D.C. Rupainwar, V.N. Singh, As(III) removal from aqueous solution by adsorption, Water Air Soil Poll. 42 (1988) 373–386.

[19] M.L. Pierce, C.B. Moore, Adsorption of arsenite on amorphous iron hydroxide from dilute aqueous solution, Environ. Sci. Technol. 14 (1980) 214–216.

[20] S. Maeda, A. Ohki, S. Saikoji, K. Naka, Iron (III) hydroxide-loaded coral limestone as an adsorbent for arsenic (III) and arsenic (V), Sep. Sci. Technol. 27 (1992) 681–689.

[21] A. Joshi, M. Chaudhuri, Removal of arsenic from ground water by iron oxide-coated sand, J. Environ. Eng.-ASCE 122 (1996) 769–771.

[22] V.K. Gupta, V.K. Saini, N. Jain, Adsorption of As(III) from aqueous solutions by iron oxide-coated sand, J. Colloid Interf. Sci. 288 (2005) 55–60.

[23] S. Kuriakose, T.S. Singh, K.K. Pant, Adsorption of As(III) from aqueous solution onto iron oxide impregnated activated alumina, Water Qual. Res. J. Can. 39 (2004) 258–266.

[24] B. Petrusevski, J. Boere, S.M. Shahidullah, S.K. Sharma, J.C. Schippers, Adsorbent-based point-of-use system for arsenic removal in rural areas, J. Water SRT–Aqua 51 (2002) 135–144.

[25] S. Bang, G.P. Korfiatis, X. Meng, Removal of arsenic from water by zero-valent iron, J. Hazard. Mater. 121 (2005) 61–67.

[26] H.-L. Lien, R.T. Wilkin, High-level arsenite removal from groundwater by zero-valent iron, Chemosphere 59 (2005) 377–386.

[27] N.P. Nikolaidis, G.M. Dobbs, J.A. Lackovic, Arsenic removal by zero-valent iron: field, laboratory and modeling studies, Water Res. 37 (2003) 1417–1425.

[28] S. Kundu, A.K. Gupta, Adsorptive removal of As(III) from aqueous solution using iron oxide coated cement (IOCC): evaluation of kinetic, equilibrium and thermodynamic models, Sep. Purif. Technol. 51 (2006) 165–172.

[29] V.C. Taty Costodes, H. Fauduet, C. Porte, A. Delacroix, Removal of Cd(II) and Pb(II) ions, from aqueous solutions, by adsorption onto sawdust of *Pinus sylvestris*, J. Hazard. Mater. 105 (2003) 121–142.

[30] R.A. Hutchins, New simplified design of activated carbon system, Am. J. Chem. Eng. 80 (1973) 133–138.

[31] A.S. Michaels, Ind. Eng. Chem. 44 (1952) 1922, as cited in L.D. Benefield, J.F. Judkins Jr., B.L. Weand, Process Chemistry for Water and Wastewater Treatment, Prentice-Hall, Inc., Englewood Cliffs, New Jersey, 1982.

[32] M.J. Humenick, Water and Wastewater Treatment: Calculations for Chemical and Physical processes, Marcel Dekker, Inc., New York, 1977, as cited in L.D. Benefield, J.F. Judkins Jr., B.L. Weand, Process chemistry for water and Wastewater Treatment, Prentice-Hall, Inc., Englewood Cliffs, New Jersey, 1982.

[33] W.J. Weber Jr., Physicochemical Processes for Water Quality Control, Wiley–Interscience, New York, 1972.

[34] H.C. Thomas, Heterogeneous ion exchange in a flowing system, J. Am. Chem. Soc. 66 (1944) 1664–1666.

[35] Y.H. Yoon, J.H. Nelson, Application of gas adsorption kinetics. 1. A theoretical model for respirator cartridge service time, Am. Ind. Hyg. Assoc. J. 45 (1984) 509–516.

[36] S. Kundu, A.K. Gupta, Investigations on the adsorption efficiency of iron oxide coated cement (IOCC) towards As(V)—kinetics, equilibrium and thermodynamic studies, Colloids Surf. A Physicochem. Eng. Aspects 273 (2006) 121–128.

[37] L.S. Clesceri, A.E. Greenberg, A.D. Eaton, *APHA*, Standard Methods for the Examination of Water and Wastewater, 20th ed., APHA, Washington, DC, 1998.

[38] WHO Guidelines for Drinking-water Quality, 2nd ed., vol. 1, 1993.

[39] WHO Guidelines for Drinking-water Quality, 3rd ed., vol. 1, 2004.

[40] Z. Aksu, F. Gönen, Biosorption of phenol by immobilized activated sludge in a continuous packed bed: prediction of breakthrough curves, Proc. Biochem. 39 (2004) 599–613.

[41] S.D. Faust, O.M. Aly, Adsorption Processes for Water Treatment, Butterworth Publishers, USA, 1987.

[42] G.S. Bohart, E.Q. Adams, Behavior of charcoal towards chlorine, J. Am. Chem. Soc. 42 (1920) 523–529.

[43] V.J.P. Poots, G. McKay, J.J. Healy, The removal of acid dye from effluent using natural adsorbents—I peat, Water Res. 10 (1976) 1061–1066.